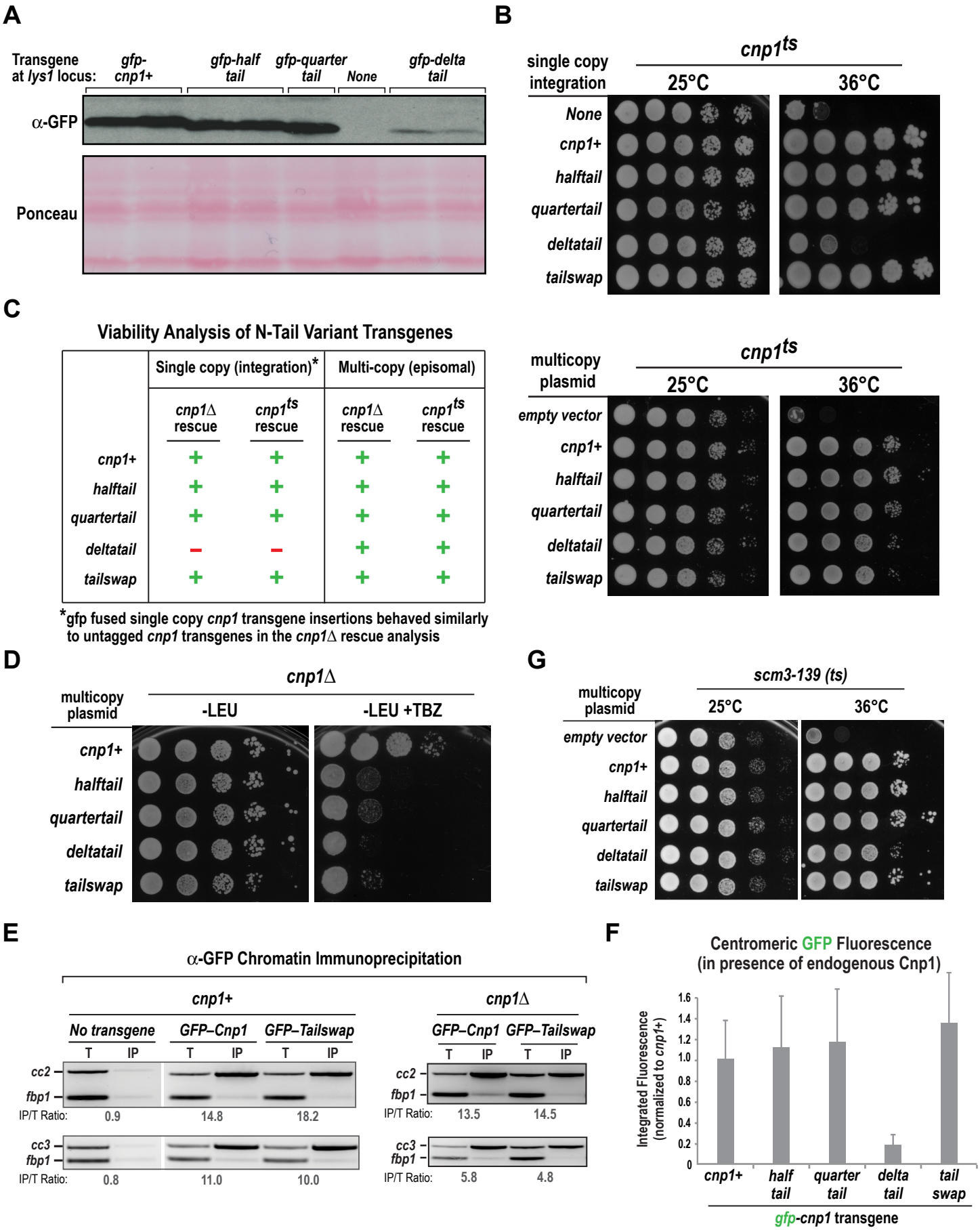
A
Transgene at lys1 locus:
gfp-cnp1+
gfp-half tail
gfp-quarter tail
None
gfp-delta tail
α-GFP
Ponceau
B
single copy integration
cnp1ts
25°C
36°C
None
cnp1+
halftail
quartertail
deltatail
tailswap
C
Viability Analysis of N-Tail Variant Transgenes
Single copy (integration)*
Multi-copy (episomal)
cnp1Δ rescue
cnp1ts rescue
cnp1Δ rescue
cnp1ts rescue
cnp1+ + + + +
halftail + + + +
quartertail + + + +
deltatail − − + +
tailswap + + + +
*gfp fused single copy cnp1 transgene insertions behaved similarly to untagged cnp1 transgenes in the cnp1Δ rescue analysis
multicopy plasmid
cnp1ts
25°C
36°C
empty vector
cnp1+
halftail
quartertail
deltatail
tailswap
D
cnp1Δ
multicopy plasmid
-LEU
-LEU +TBZ
cnp1+
halftail
quartertail
deltatail
tailswap
G
scm3-139 (ts)
multicopy plasmid
25°C
36°C
empty vector
cnp1+
halftail
quartertail
deltatail
tailswap
E
α-GFP Chromatin Immunoprecipitation
cnp1+
No transgene
GFP–Cnp1
GFP–Tailswap
cnp1Δ
GFP–Cnp1
GFP–Tailswap
T
IP
cc2
fbp1
IP/T Ratio: 0.9 14.8 18.2
IP/T Ratio: 13.5 14.5
cc3
fbp1
IP/T Ratio: 0.8 11.0 10.0
IP/T Ratio: 5.8 4.8
F
Centromeric GFP Fluorescence
(in presence of endogenous Cnp1)
Integrated Fluorescence (normalized to cnp1+)
1.6
1.4
1.2
1.0
0.8
0.6
0.4
0.2
0
cnp1+
half tail
quarter tail
delta tail
tail swap
gfp-cnp1 transgene

A

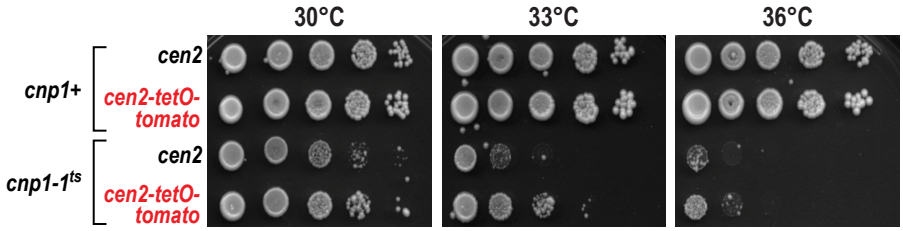

B

Mating Assay Test for Synthetic Lethality*

Array	N-Tail Variant	N-Tail Variant Colonies (Ratio relative to total)
no TetO array	GFP-Cnp1	0.44
	GFP-Tailswap	0.27
pericen1-tetO-tomato	GFP-Cnp1	0.51
	GFP-Tailswap	0.21
cen2-tetO-tomato	GFP-Cnp1	0.20
	GFP-Tailswap	0.007

*see Table S1 (Sets B,D & E)

C

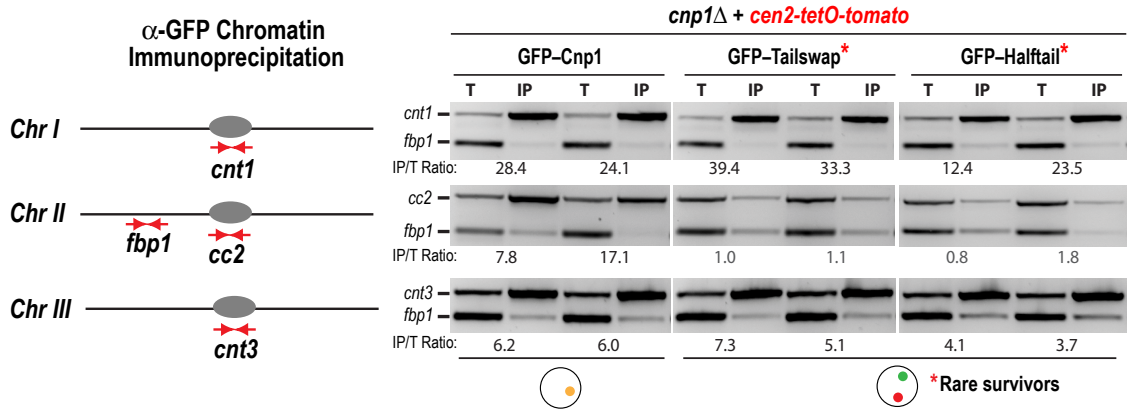

D

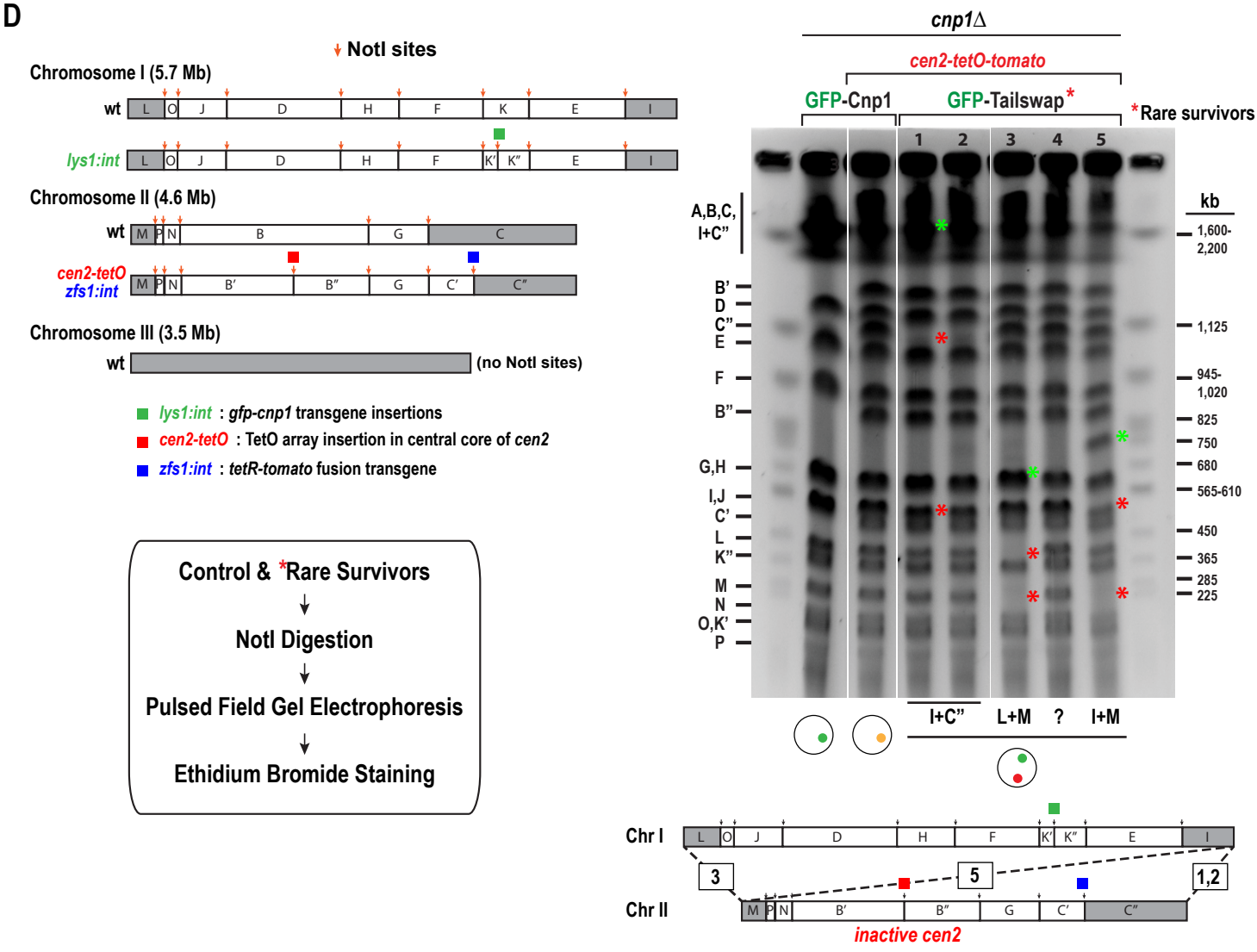

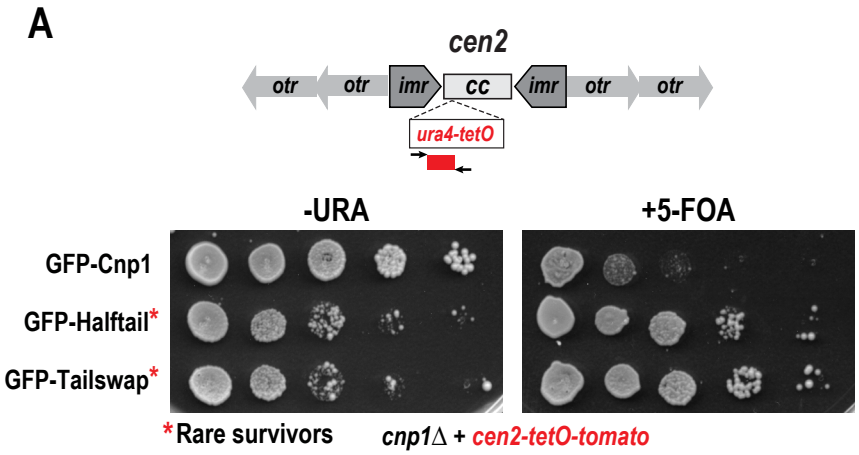
A
cen2
otr
otr
imr
cc
imr
otr
otr
ura4-tetO
-URA
+5-FOA
GFP-Cnp1
GFP-Halftail*
GFP-Tailswap*
*Rare survivors
cnp1Δ + cen2-tetO-tomato

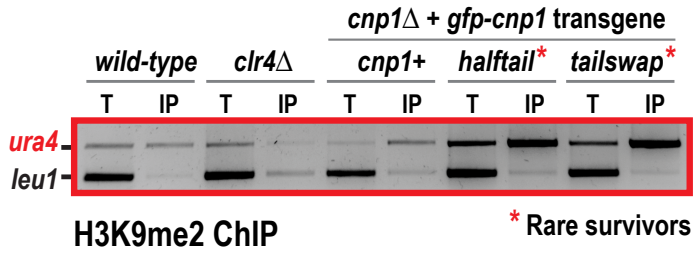
B
cnp1Δ + gfp-cnp1 transgene
wild-type
clr4Δ
cnp1+
halftail*
tailswap*
T
IP
T
IP
T
IP
T
IP
T
IP
ura4
leu1
H3K9me2 ChIP
* Rare survivors

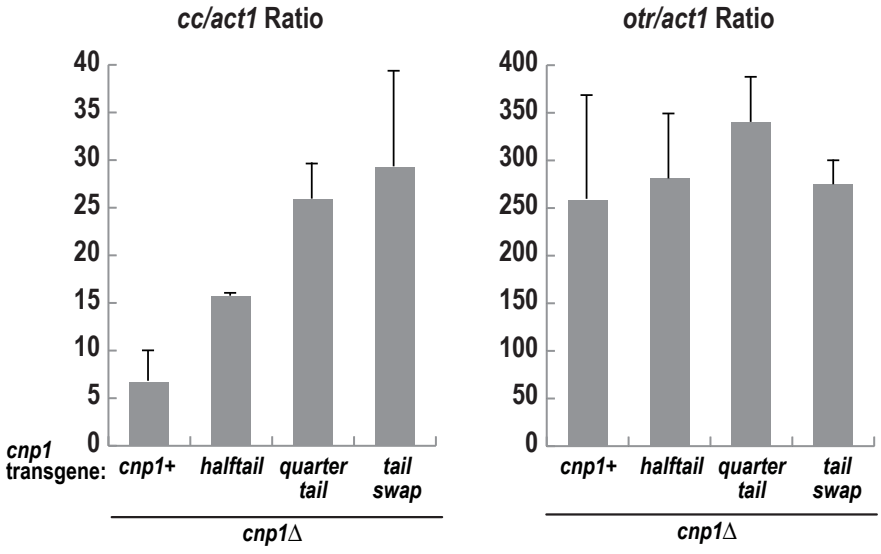
C
H3K9me2 ChIP-qPCR
cc/act1 Ratio
otr/act1 Ratio
40
35
30
25
20
15
10
5
0
400
350
300
250
200
150
100
50
0
cnp1 transgene:
cnp1+
halftail
quarter tail
tail swap
cnp1Δ

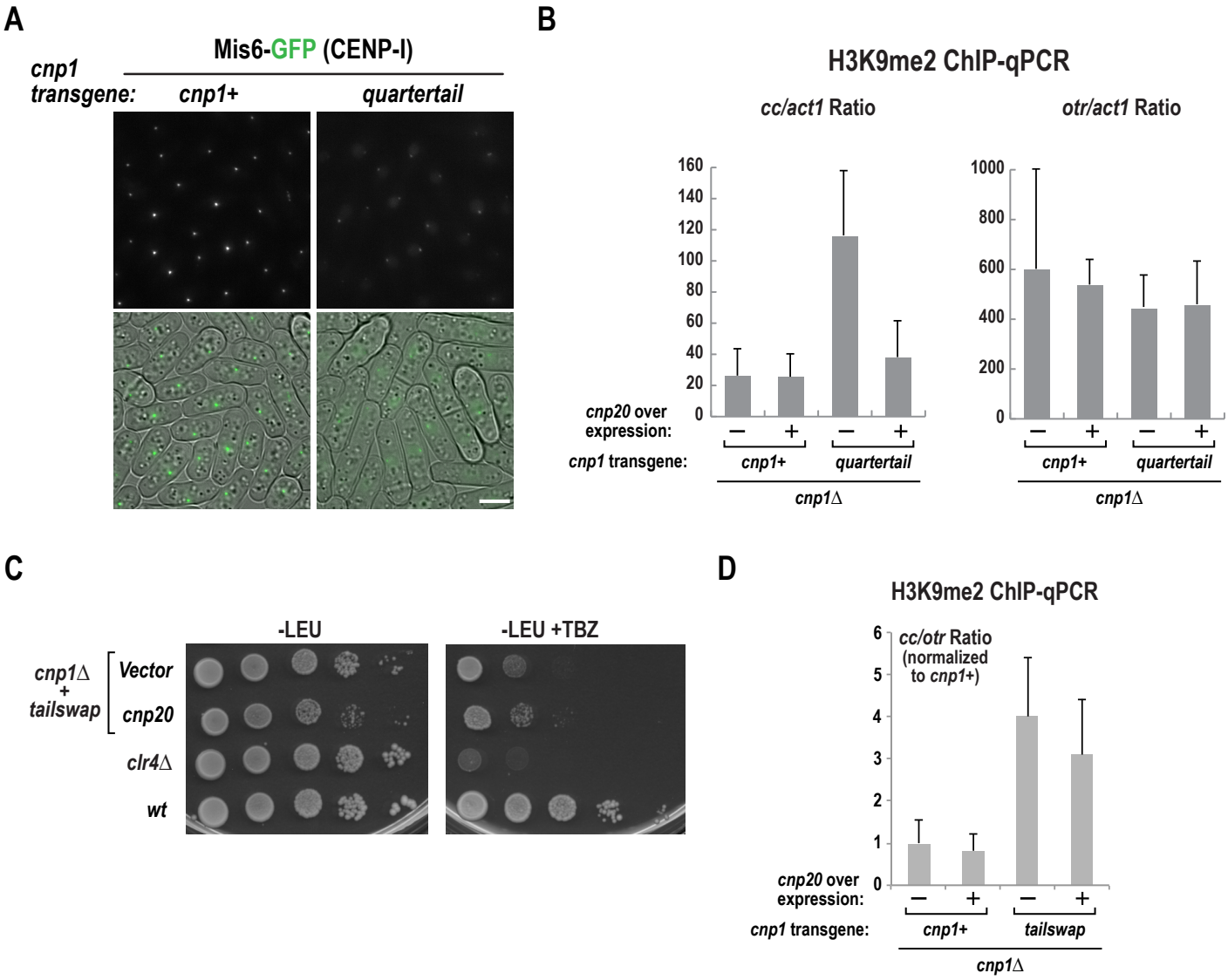
A
Mis6-GFP (CENP-I)
cnp1 transgene:
cnp1+
quartertail
B
H3K9me2 ChIP-qPCR
cc/act1 Ratio
otr/act1 Ratio
160
140
120
100
80
60
40
20
0
1000
800
600
400
200
0
cnp20 over expression:
cnp1 transgene:
cnp1+
quartertail
cnp1Δ
C
-LEU
-LEU +TBZ
cnp1Δ + tailswap
Vector
cnp20
clr4Δ
wt
D
H3K9me2 ChIP-qPCR
cc/otr Ratio (normalized to cnp1+)
6
5
4
3
2
1
0
cnp20 over expression:
cnp1 transgene:
cnp1+
tailswap
cnp1Δ

SUPPLEMENTAL FIGURE LEGENDS

Suppl. Figure 1 (Related to Figure 1). Characterization of Cnp1 N-tail variants.

A. Anti-GFP immunoblot of indicated GFP-tagged Cnp1 N-tail variants. Ponceau staining is shown as a loading control.

B. Rescue of *cnp1 ts* (temperature-sensitive) mutants by Cnp1 N-tail variants. Top: *cnp1-76* (ts) rescue by single copy integrations at *lys1* expressed under endogenous *cnp1* promoter. Bottom: Rescue of *cnp1-1* (ts) by Cnp1 N-tail variants expressed under the *nmt1* promoter in multicopy pREP81 plasmids. A ten-fold dilution series is shown for each strain.

C. Summary of the viability rescue assays conducted for Cnp1 N-tail variants.

D. Overexpression of Cnp1 N-tail variants does not rescue their TBZ sensitivity. Serial dilution (10-fold) of *cnp1Δ* cells expressing Cnp1 N-tail variants on multicopy plasmid pREP81 were plated on minimal media or without the addition of 10 µg/ml TBZ. Growth was assayed at 30°C.

E. Anti-GFP ChIP of wild type and *cnp1Δ* cells expressing indicated GFP-Cnp1 variants (the absence of any transgene serves as a control). Enrichment at centromeres (*cc2* and *cc3* products) was determined by comparison with input DNA, relative to the control non-centromeric locus *fbp1*.

F. Fluorescence intensity at centromeres of indicated GFP-tagged Cnp1 variants integrated at single-copy in a *cnp1+* strain. Error bars represent the SD (n>100 per strain).

G. Rescue of *scm3-139* ts cells (10-fold dilution series) by Cnp1 N-tail variants expressed on the multi-copy plasmid pREP81.

Suppl. Figure 2 (Related to Figure 2). Analysis of the Cnp1 N-tail variant – *cen2-tetO-tomato* synthetic lethal interaction.

A. *cen2-tetO-tomato* does not affect the temperature sensitivity of the *cnp1-1^{ts}* mutant. 10-fold serial dilutions of *cnp1Δ* cells expressing *cnp1+* or *cnp1-1^{ts}* harboring either *cen2* or *cen2-tetO-tomato* were plated on rich YES medium and incubate at various temperatures as indicated.

B. GFP-Tailswap is synthetic lethal with a centromeric but not a pericentromeric TetO array. The genetic interaction between GFP-Cnp1 or GFP-Tailswap and indicated *tetO-tomato* arrays was measured employing the assay depicted in *Fig. 2A*. Please see *Table S1* for further details.

C. Evidence for loss of *cen2* identity, based on anti-GFP ChIP, in rare survivors expressing either GFP-Tailswap or GFP-Halftail as the sole source of Cnp1 and harboring *cen2-tetO-tomato*. Enrichment at centromeres (*cnt1, cc2* and *cnt3* products) was estimated based on comparison with input DNA relative to the control non-centromeric locus *fbp1*.

D. *Not*I digestion-based analysis of chromosome fusions. Schematic on the left indicates the *Not*I digestion pattern for the strain harboring the indicated insertions (*red, green and blue squares*). Chromosomal DNA samples digested with *Not*I from indicated strains were analyzed by pulsed-field gel electrophoresis (*right*). Green asterisks indicate new bands originated by the fusion of two missing bands, indicated as red asterisks. Schematics below summarize the 4 fusions observed in 4/5 GFP-Tailswap survivors. For one survivor (#4), no clear alteration in the band pattern was observed, suggesting either a fusion with Chr III or formation of a neocentromere.

Suppl. Figure 3 (Related to Figure 3). Analysis of H3K9me2 at the central core of the centromere.

A. To assess silencing of a *ura4* marker adjacent to the *tetO array* in the central core of *cen2*, cells were serially diluted (10-fold) on minimal medium lacking uracil (-URA) and counter-selective 5-FOA medium. Improved growth on 5-FOA indicates hyper-silencing of the *ura4* marker cassette in the rare survivors with inactivated *cen2*.

B. ChIP with H3K9me2 antibody was performed on the cells used in the plating assay in *Fig. S3A*. Wildtype and *clr4Δ* controls are also shown. The amount of H3K9me2 enrichment at the *ura4* cassette was compared to the non-centromeric control *leu1.* The results show strong H3K9me2 enrichment at the central core of the inactive centromere.

C. ChIP-qPCR analysis of H3K9me2 from *Fig. 3C* replotted to show enrichment at heterochromatic outer repeats (*otr*) and centromeric central core 1 & 3 (*cc*) relative to the non-centromeric control *act1*. Error bars represent the SD (n=3)

Suppl. Figure 4 (Related to Fig. 4). Analysis of Mis6/CENP-I localization and suppression of H3K9me2 by Cnp20/CENP-T overexpression.

A. Representative images of Mis6-GFP in the indicated strains. Scale bar represents 5 μm. See quantification in **Fig. 4B**.

B. ChIP-qPCR analysis of H3K9me2 from *Fig. 4D* replotted to show enrichment at heterochromatic outer repeats (*otr*) and centromeric central core 1 & 3 (*cc*) relative to the non-centromeric control *act1*. Error bars represent the SD (n=3)

C. Serial dilutions of Tailswap strains harboring empty or Cnp20-overexpressing multicopy pREP1 plasmid were plated on minimal medium lacking leucine (PMG –LEU), with or

without 15 µg/ml TBZ, and grown at 30°C. A ten-fold dilution series is shown for each strain. *clr4Δ* serves as a TBZ-sensitive control.

D. ChIP-qPCR with H3K9me2 antibody for the indicated conditions. The normalized ratio of products from Cnp1-enriched regions (*cc*) and heterochromatic outer repeats (*otr*) is displayed. Error bars represent the SD (n=3).

Table S2. List of yeast strains used in this study.

Table S1. Analysis of genetic interactions between Cnp1 N-tail variants and *tetO-tomato* insertions

Relevant genotype	Method	Variant	Strains	Ratio	N
Set A: unaltered *cen2* control	G418 25°C & 36°C:	***GFP-cnp1+***	P770 x Q128	**0.20**	1009
lys1+>cnp1-ts cnp1::KAN	# colonies 36°C		P771 x Q128	**0.62**	533
X	# colonies 25°C	***GFP-tailswap***	P770 x Q133	**0.14**	1729
*lys1+>**variant***			P771 x Q133	**0.33**	410
		GFP-cnp1+	P871 x P204	**0.19**	884
			P871 x P955	**0.22**	980
			P871 x P204	**0.21**	1541
Set B: *cen2-tetO-tomato*			P871 x P275	**0.004**	1896
lys1+>cnp1-ts cnp1::KAN	G418 25°C & 36°C:	***GFP-tailswap***	P871 x P957	**0.01**	2490
cen2-tetO tetR-tomato	# colonies 36°C		P871 x P275	**0.007**	1611
X	# colonies 25°C				
*lys1+>**variant***		***GFP-halftail***	P871 x P214	**0.008**	1227
cen2-tetO tetR-tomato			P871 x P215	**0.001**	1621
		GFP-quartertail	P871 x P216	**0.02**	1451
			P871 x P693	**0.001**	1229
		GFP-cnp1+	Q166 x Q175	**0.50**	587
Set C: *cen2-tetO-tomato clr4Δ*			Q166 x Q176	**0.74**	1005
clr4Δ lys1+>cnp1-ts cnp1::KAN					
cen2-tetO tetR-tomato	G418 25°C & 36°C:		Q169 x Q175	**0.003**	174
X	# colonies 36°C		Q169 x Q176	**0.03**	369
*clr4Δ lys1+>**variant***	# colonies 25°C	***GFP-tailswap***	Q170 x Q175	**0.01**	1149
cen2-tetO tetR-tomato			Q170 x Q176	**0.009**	964
			Q171 x Q175	**0.01**	288
			Q171 x Q176	**0.002**	297

		GFP-cnp1+	Q087 x Q128	**0.44**	157
Set D: unaltered *cen1* control					
lys1+>cnp1+>>ade6+ cnp1::KAN	G418 low ade 30°C:	***cnp1+***	Q087 x Q129	**0.40**	433
ade6-210	# red colonies				
*X lys1+>**variant***	# total colonies		Q087 x Q131	**0.24**	167
ade6-210		***GFP-tailswap***	Q087 x Q132	**0.28**	249
			Q087 x Q133	**0.28**	298
Set E: *pericen1-tetO-tomato*		***GFP-cnp1+***	P968 x Q001	**0.49**	309
*lys1+>**variant**>>ade6+* ade6-210*			P967 x Q005	**0.52**	248
pericen1-tetO tetR-tomato	G418 low ade 30°C:				
X	# white colonies	***GFP-tailswap***	P968 x Q003	**0.23**	71
lys1+>cnp1+ cnp1::KAN	# total colonies		P967 x Q007	**0.20**	105
ade6-210 tetR-tomato					

***** *lys1* locus is linked to *cen1* (<1cM). Therefore, *variant>>ade6+* is also linked to *pericen1-tetO*

Table S3. Oligonucleotides used in this study

Primer	Sequence	PCR product	Figure
HDF-37	TTCGACAACAGGATTACGACC	*ura4*	S3B
HDF-39	GAGGGGATGAAAAATCCCAT	*ura4*	S3B
HDF-47	AATGACAATTCCCCACTAGCC	*fbp1*	3A, S1F, S2C
HDF-48	ACTTCAGCTAGGATTCACCTGG	*fbp1*	3A, S1F, S2C
HDF-138	GCTTTATCATAGTATTTTAGGC	*cnt1*	S2C
HDF-139	AATACTTGGTATGTTAAAGTGG	*cnt1*	S2C
HDF-142	ATTCAGGATGCTTTCAGTTG	*cnt3*	S1F, S2C
HDF-143	AATCTAAGGAACCCGGTAAG	*cnt3*	S1F, S2C
HDF-202	GACCTAGAAGTAAAATTCGT	*otr*	3A
HDF-203	GCGGTTGTTTGGCACTGAATGTAA	*otr*	3A
HDF-204	TTTGGTCAAGAGCCCTCGTA	*leu1*	3A, S3B
HDF-205	TAGAAGCCTCACCTCCCAAA	*leu1*	3A, S3B
HDF-210	CGTTCATACAGATGACTTTCC	*cc2*	3A, S1F, S2C
HDF-211	CCAACTGATCCTTCAAACTAC	*cc2*	3A, S1F, S2C
HDF-245	CAGACAATCGCATGGTACTATC	qPCR *cc*	3C, 4C, S3C, S4B, S4D
HDF-246	AGGTGAAGCGTAAGTGAGTG	qPCR *cc*	3C, 4C, S3C, S4B, S4D
HDF-323	AACCCTCAGCTTTGGGTCTT	qPCR *act1*	3C, 4C, S3C, S4B
HDF-324	TTTGCATACGATCGGCAATA	qPCR *act1*	3C, 4C, S3C, S4B
HDF-325	AATTGTGGTGGTGTGGTAATAC	qPCR *otr*	3C, 4C, S3C, S4B, S4D
HDF-326	GGGTTCATCGTTTCCATTCAG	qPCR *otr*	3C, 4C, S3C, S4B, S4D

SUPPLEMENTAL EXPERIMENTAL PROCEDURES

Strain and Plasmid Construction

Standard procedures were used for fission yeast growth, genetics and manipulations [S1]. *S. pombe* strains used in this study are listed in **Table S2**. Cells were grown at 30°C unless otherwise stated. Cnp1 N-tail variants were obtained by a combination of PCR and subcloning into pS2 [S2] and LEU2-marked pREP81 plasmids. *cnp20* was PCR-amplified from genomic DNA and cloned into pREP1 plasmid. pS2-based plasmids were linearized with *Nsi*I and introduced by transformation at *lys1+* locus. Strains expressing Cnp1 N-tail variants as unique source of Cnp1 were isolated as described [S3]. The following arrays, gene fusions and mutant alleles were previously described: *cen2-tetO-Tomato* [S4], *pericen2-lacO-GFP* (cen2-D107 [S5]), *cnp20-GFP* and *cnp3-Tomato* [S6], *mis6-GFP* [S7]), *ndc80-GFP* [S8]), *cnp1-1* [S9], *cnp1-76* [S10], *scm3-139* [S11]) and *nda3-KM311* [S12]. *pericen1L-ade6+* and *pericen1R-tetO* strains (gifts from Robin Allshire) harbor insertions of *ade6+* gene and a 5.2 kb tetO array at the pericentromeric *Xho*I sites, left and right hand side, respectively.

Mating-based random sporulation assay

To determine if the combination of a specific N-tail variant and the *cen2-tetO* array insertion resulted in synthetic lethality, we measured the ratio of the number of colonies at 36°C (which prevents growth of spores that inherited the *cnp1-1*^{ts} mutant) versus 25°C as follows: Briefly, two types of parental strains were mated and sporulated: i) *cnp1*Δ strains rescued by a *cnp1-1* temperature-sensitive (*cnp1-1*^{ts}) mutant transgene integrated at the *lys1* locus and, ii) wild-type strains containing *gfp-cnp1* N-tail variant transgenes also integrated at the

lys1 locus. In addition, both parental strains harbored either an unaltered centromere 2 (*cen2*) or a centromere 2 with a *tetO* array insertion in the central core (*cen2-tetO-tomato*). Spores generated after mating were selected for *cnp1*Δ (based on resistance to G418), making the *lys1*-integrated transgene the sole source of Cnp1.

PFGE

Pulsed-field gel electrophoresis was performed as described [S13].
CHEF-DR III and CHEF-DR (Biorad) were used for running untreated (48 h run) and *Not*I-digested plugs (24 h run), respectively.

Spindle checkpoint assay

nda3-KM311 cells were grown in YES at 30°C to mid log phase then shifted to the non-permissive temperature (18°C). Samples were taken every 2 hrs for 8 hrs, fixed in ice cold methanol, then stained with DAPI (1μg/ml) and calcofluor (15μg/ml).

Imaging

Cells were grown and mounted as described [S3]. Images were acquired either on spinning-disc microscope with a 100X 1.4NA Plan Apochromat oil lens or a Delta Vision Elite microscope (Applied Precision) with a 100X 1.35 NA oil lens (Olympus). Time-lapse experiments were performed on a Deltavision (Applied Precision) microscope with an Olympus 60X, 1.4NA oil lens. Further image processing, including maximum intensity projections and measurement of fluorescence intensities, was performed using ImageJ (National Institutes of Health). Background-subtracted centromere intensity measurements were performed as described [S14].

Chromatin immunoprecipitation (ChIP)

Cells were grown in rich media or PMG –LEU when plasmid selection was required. Anti-GFP (A11122, Invitrogen) and anti-H3K9me2 (ab1220, Abcam) were used in ChIPs as described [S3, S15]. Oligonucleotides employed in semiquantitative duplex PCR and qPCR are listed in **Table S3**.

ChIP-seq

A described method [S16] with minor modifications was used for ChIP-seq. Briefly, the cells were lysed with zymolase and chromatin was sonicated to a range of 200-1000 bases. Approximately 500 ng of chromatin per sample was used. ChIP-seq data was aligned to the following assembly ASM294v2_19 with BWA. Only those reads with a MAPQ of 10 or greater were used; MAPQ of 10 or greater indicates that reads map uniquely. The parameters used for the mapping were 25 base pair reads, allowing 2 mismatches per read. Because sequencing can easily be saturated with a relatively small genome such as fission yeast, 1,000,000 reads were randomly selected to perform peak calling and generate wig files. For the .wig files, the data was binned into 200 bases. Sequencing data are available at the NCBI Gene Expression Omnibus (GEO) repository under the accession number GSE63350.

SUPPLEMENTAL REFERENCES

S1. Sabatinos, S.A., and Forsburg, S.L. (2010). Molecular genetics of Schizosaccharomyces pombe. Methods in enzymology *470*, 759-795.

S2. Takayama, Y., Sato, H., Saitoh, S., Ogiyama, Y., Masuda, F., and Takahashi, K. (2008). Biphasic incorporation of centromeric histone CENP-A in fission yeast. Molecular biology of the cell *19*, 682-690.

S3. Fachinetti, D., Folco, H.D., Nechemia-Arbely, Y., Valente, L.P., Nguyen, K., Wong, A.J., Zhu, Q., Holland, A.J., Desai, A., Jansen, L.E., et al. (2013). A two-step mechanism for epigenetic specification of centromere identity and function. Nature cell biology *15*, 1056-1066.

S4. Sakuno, T., Tada, K., and Watanabe, Y. (2009). Kinetochore geometry defined by cohesion within the centromere. Nature *458*, 852-858.

S5. Yamamoto, A., and Hiraoka, Y. (2003). Monopolar spindle attachment of sister chromatids is ensured by two distinct mechanisms at the first meiotic division in fission yeast. The EMBO journal *22*, 2284-2296.

S6. Tanaka, K., Chang, H.L., Kagami, A., and Watanabe, Y. (2009). CENP-C functions as a scaffold for effectors with essential kinetochore functions in mitosis and meiosis. Developmental cell *17*, 334-343.

S7. Saitoh, S., Takahashi, K., and Yanagida, M. (1997). Mis6, a fission yeast inner centromere protein, acts during G1/S and forms specialized chromatin required for equal segregation. Cell *90*, 131-143.

S8. Hayashi, A., Asakawa, H., Haraguchi, T., and Hiraoka, Y. (2006). Reconstruction of the kinetochore during meiosis in fission yeast Schizosaccharomyces pombe. Molecular biology of the cell *17*, 5173-5184.

S9. Takahashi, K., Chen, E.S., and Yanagida, M. (2000). Requirement of Mis6 centromere connector for localizing a CENP-A-like protein in fission yeast. Science *288*, 2215-2219.

S10. Pidoux, A.L., Richardson, W., and Allshire, R.C. (2003). Sim4: a novel fission yeast kinetochore protein required for centromeric silencing and chromosome segregation. The Journal of cell biology *161*, 295-307.

S11. Pidoux, A.L., Choi, E.S., Abbott, J.K., Liu, X., Kagansky, A., Castillo, A.G., Hamilton, G.L., Richardson, W., Rappsilber, J., He, X., et al. (2009). Fission yeast Scm3: A CENP-A receptor required for integrity of subkinetochore chromatin. Molecular cell *33*, 299-311.

S12. Hiraoka, Y., Toda, T., and Yanagida, M. (1984). The NDA3 gene of fission yeast encodes beta-tubulin: a cold-sensitive nda3 mutation reversibly blocks spindle formation and chromosome movement in mitosis. Cell *39*, 349-358.

S13. Nicolas, E., Yamada, T., Cam, H.P., Fitzgerald, P.C., Kobayashi, R., and Grewal, S.I. (2007). Distinct roles of HDAC complexes in promoter silencing, antisense suppression and DNA damage protection. Nature structural & molecular biology *14*, 372-380.

S14. Hoffman, D.B., Pearson, C.G., Yen, T.J., Howell, B.J., and Salmon, E.D. (2001). Microtubule-dependent changes in assembly of microtubule motor proteins and mitotic spindle checkpoint proteins at PtK1 kinetochores. Molecular biology of the cell *12*, 1995-2009.

S15. Cam, H.P., Sugiyama, T., Chen, E.S., Chen, X., FitzGerald, P.C., and Grewal, S.I. (2005). Comprehensive analysis of heterochromatin- and RNAi-mediated epigenetic control of the fission yeast genome. Nature genetics *37*, 809-819.
S16. Hawkins, R.D., Hon, G.C., Lee, L.K., Ngo, Q., Lister, R., Pelizzola, M., Edsall, L.E., Kuan, S., Luu, Y., Klugman, S., et al. (2010). Distinct epigenomic landscapes of pluripotent and lineage-committed human cells. Cell stem cell *6*, 479-491.